An Analysis of the Voltammetric Adsorption Waves of Methyl Viologen

Katsuyoshi KOBAYASHI,* Fumiaki FUJISAKI, Toshifumi YOSHIMINE, and Katsumi NIKI
Department of Electrochemistry, Faculty of Engineering, Yokohama National University, Tokiwadai, Hodogaya-ku, Yokohama 240
(Received March 14, 1986)

The electrochemical behavior of 1,1′-dimethyl-4,4′-bipyridinium dichloride (methyl viologen, MV) is complicated with the strong adsorption of both the oxidized (MV^{2+}) and the reduced ($MV^{+\cdot}$) forms of MV on a mercury electrode. MV^{2+} adsorbs on the electrode with a flat orientation at more positive potentials than the potential of zero charge of the mercury electrode. $MV^{+\cdot}$ adsorbs on the electrode with a vertical orientation at more negative potentials than the formal potential of the $MV^{2+/+\cdot}$ couple, $(E^{0'})_{MV}$. It is probable that the change in the orientation of the adsorbed $MV^{+\cdot}$ from flat to vertical with the increase in the $MV^{+\cdot}$ concentration in the vicinity of the $(E^{0'})_{MV}$ leads to a strongly attractive interaction between the adsorbed $MV^{+\cdot}$ molecules and a sharp voltammetric adsorption peak results at higher concentrations of MV^{2+}.

Methyl viologen has been widely used as one of the active herbicides, the "paraquat" family.[1] This herbicidal activity originates from the formation of the cation radical of methyl viologen.[2,3]

MV^{2+} is reduced in two steps. The first step is a reversible one-electron transfer with a very negative half-wave potential, −(0.68—0.69) V vs. a saturated calomel electrode (SCE).[4,5] The reduction of MV^{2+} to the methyl viologen cation radical, which is relatively stable in an oxygen-free solution,[6-8] causes a marked color change. MV acts as a good electron-transfer mediator for biological systems.[5,9] These properties lead to the applications of MV to photoelectrodes,[10-14] electrochromisms,[15-19] and electrocatalyses.[20-24]

The electrochemical behavior of MV itself is complicated by the strong adsorption of both MV^{2+} and $MV^{+\cdot}$ molecules on a mercury electrode. Pospisil et al.[3,25] and Grachev et al.[8] have reported on the analysis of the adsorption waves of MV by means of classical d.c. and a.c. polarographic techniques. Recently, resonance and surface enhanced Raman scattering spectroscopies[26,27] and UV-visible reflectance spectroscopy[28] have been used for in situ studies of the redox behavior of adsorbed methyl viologen molecules on silver and platinum electrodes. However, the conformation of both the adsorbed MV^{2+} and $MV^{+\cdot}$ molecules at the electrode surface has not yet been discussed in detail.

Wopshall and Shain[29] showed in the simulation of cyclic voltammograms that a sharp adsorption wave appears when the adsorption coefficient varies with the electrode potential. In many redox systems, similar sharp adsorption waves have been reported.[30-35] In classical d.c. polarograms of Methylene Blue, the half-wave potential ($E_{1/2}$) of the single adsorption wave depends upon its concentration, while the $E_{1/2}$ of the prewave has a constant value when a double wave is observed.[36] Laviron[37] has shown that the dependence of $E_{1/2}$ on the concentration of the reactant is due to the interaction between the adsorbed redox molecules, provided that the adsorption coefficient is large enough. Flanagan et al.[38,39] discussed the effects of reactant and product adsorption in the digital simulation of pulse polarograms.

In the present work, we have found several unusual adsorption phenomena of methyl viologen using the normal pulse (NPP), differential pulse (DPP), and a.c. polarographic techniques. That is, in NPP, 1) a single wave is observed at concentrations lower than 0.5 mM, and a sharp prewave appears at concentrations higher than 0.5 mM for the forward scan. However, a sharp postwave appears over the whole concentration range investigated for the reverse scan. 2) The half-wave potential of the single wave ($E_{1/2,s}$) is about 0.2 V more positive than the $(E^{0'})_{MV}$ and depends upon both the sampling time (t_s) and the initial potential (E_{in}) of NPP. 3) The cathodic prewave on the forward scan always appears at a more negative potential than the anodic postwave on the reverse scan. At concentrations lower than 0.5 mM, the $E_{1/2,s}$ on the forward scan is much more positive than the peak potential (E_p) of the postwave on the reverse scan. 4) On the forward scan, the $E_{1/2,s}$ in the lower concentration range of (0.01—0.5) mM shifts toward negative potentials with the increase in the MV^{2+} concentration in contrast to the positive shift of the E_p of the prewave in the higher concentration range (>0.5 mM). On the reverse scan, the E_p of the postwave always shifts toward positive potentials with an increase in the MV^{2+} concentration.

The surface concentrations of adsorbed MV^{2+} and $MV^{+\cdot}$ molecules, as determined by the present potential-step chroncoulometry, indicate that the orientation of MV^{2+} molecules adsorbed on a mercury electrode is different from that of $MV^{+\cdot}$ molecules.

The peculiar adsorption behavior of methyl viologen can be explained by considering an orientation change in the adsorbed redox species.

Experimental

Materials. The 1,1′-dimethyl-4,4′-bipyridinium dichloride (BDH Chemical, Ltd) and 4,4′-bipyridyl (Tokyo Kasei Kogyo Co.) were of a reagent grade and were used without further purification. The phosphate buffer solution (pH 7.0) was 0.1 M (M=mol dm^{-3}) and was prepared from chemicals of the pH standard grade from Wako Pure Chemical Industries, Ltd. All the solutions were prepared from triply

distilled water.

Apparatus and Procedures. The d.c. polarographic measurements (classical d.c., tast, normal pulse, and differential pulse polarographies) were carried out with a Fuso Polarograph (Fuso and Co., Model 312) and the cyclic voltammetric measurements with a Fuso Potentiostat (Model 311) and a Fuso Potential Scanning Unit (Model 321). The a.c. polarographic measurements were carried out with a Fuso Potentiostat (Model 311), a Fuso Phase-sensitive Detector (Model 332), and a RC Oscillator (Matsushita Communication Industrial Co., Ltd, Model VP 722A). The potential-step chronocoulometric measurements were carried out with a Transient Converter (Riken Denshi Co., Ltd, Model TCA 1000) and a Fuso Potentiostat (Model 311 S2). The concentration of MV in the stock solution was determined spectrophotometrically (molar absorption coefficient at 605 nm, ε_{605}=12400 $M^{-1}cm^{-1}$)[5] with a UV-visible Recording Spectrophotometer (Shimadzu Corporation, Model UV2).

A two-compartment water-jacketed electrochemical cell was used; the compartments were separated by porous Vycor glass so that the contamination of oxygen could be minimized. The working electrode used was a dropping mercury electrode (DME), and the flow rate of mercury was 1.335 mg s^{-1} at an open circuit in a 0.1 M phosphate buffer solution (pH 7.0). The working electrode in the cyclic voltammetry was a Metrohm hanging mercury drop electrode (25.6×10^{-3} cm^2). The counter electrode was a mercury pool in the working electrode compartment. The reference electrode was a saturated calomel electrode which was separated from the working electrode compartment by porous Vycor glass. The reference electrode was coupled with a platinum wire (0.3 mm diameter) electrode in the working electrode compartment through a 0.1 μF capacitor in order to improve the response at higher frequencies in the a.c. polarographic measurements. The solution was deaerated by bubbling purified argon through the solution. All the experiments were carried out at (25±0.5) °C.

Results

Cyclic Voltammetry. Figure 1 shows some cyclic voltammograms of 1 mM MV^{2+} in 0.1 M of a phosphate buffer solution at pH 7.0. The i_p of the main wave was linear with respect to $v^{1/2}$, and the plot passed through the point of the origin, where i_p was the peak current and v the rate of the potential scan. The ratio of cathodic to anodic peak currents was almost unity. The peak-to-peak separation was about 60 mV, and the midpoint potential was −0.68 V. That is, the electrode reaction of MV in the bulk is a diffusion-controlled reversible electrode process. The prepeak shifted toward positive potentials with an increase in the concentration of MV^{2+}. The anodic postpeaks were sharper and higher than the cathodic prepeaks.

Classical d.c. Polarography. A small prewave was followed by the main wave. The $E_{1/2}$ of the main wave was −0.68 V in the concentration range of (0.4—5) mM MV^{2+}. The prewave observed at −0.62 V in 5 mM of a MV^{2+} solution shifted toward negative potentials with the decrease in the MV^{2+} concentration and merged into the main wave at concentrations below 0.25 mM.

Differential Pulse Polarography. Figure 2 shows

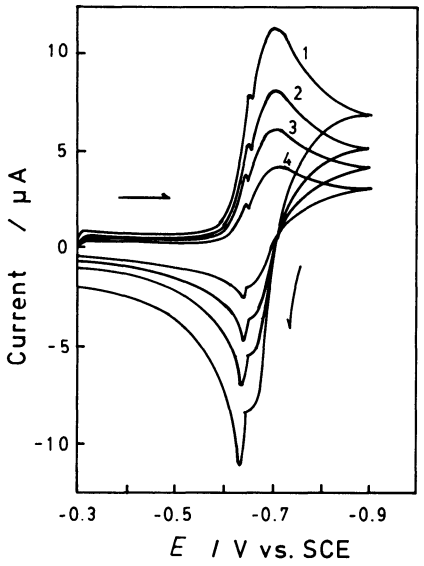

Fig. 1. Cyclic voltammograms of 1 mM MV^{2+} in a 0.1 M phosphate buffer solution (pH 7.0). Scan rates are (1): 200 mV s^{-1}, (2): 100 mV s^{-1}, (3): 50 mV s^{-1}, and (4): 20 mV s^{-1}.

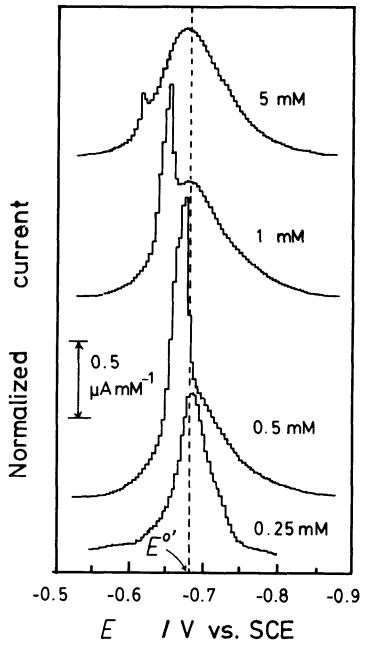

Fig. 2. Concentration dependence of differential pulse polarograms of methyl viologen in a 0.1 M phosphate buffer solution (pH 7.0). The concentrations are given on polarograms. The scan rate is 2 mV s^{-1}, the drop time 2 s, the sampling time 30 ms, and the modulation amplitude 10 mV.

the concentration dependence of the differential pulse polarograms of MV. At 0.1 mM, a single asymmetric peak was observed at −0.7 V, and the width of the peak at half height ($W_{1/2}$) was about 60 mV. At 0.25 mM, a single asymmetric peak was at −0.68 V, and $W_{1/2}$ was about 50 mV. At concentrations higher than 0.5 mM, a very sharp prepeak ($W_{1/2}$<20 mV) was separated from the main wave ($W_{1/2}$=90 mV, E_p=−0.68 V), and the

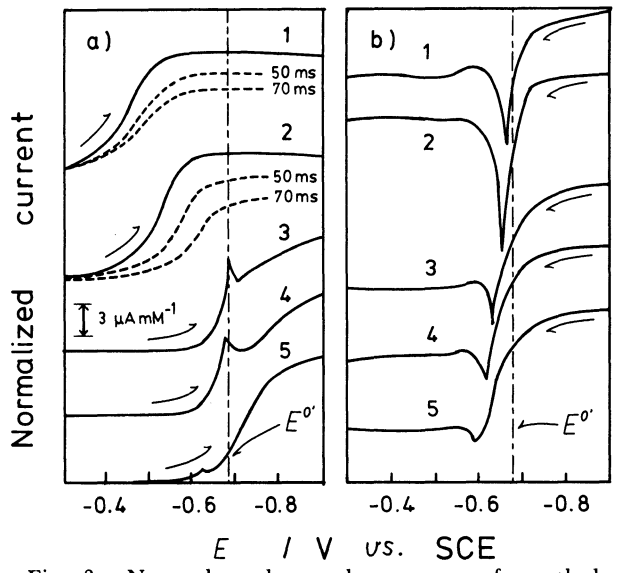

Fig. 3. Normal pulse polarograms of methyl viologen in a 0.1 M phosphate buffer solution (pH 7.0). a) On the forward scan with E_{in}=−0.3 V, and b) on the reverse scan with E_{in}=−0.9 V. The concentrations are (1): 0.1 mM, (2): 0.25 mM, (3): 0.75 mM, (4): 1 mM, and (5): 5 mM. (-----): Measured at the sampling times of 50 ms and 70 ms. t_d=2 s and t_s=30 ms.

potentials of the prepeak shifted toward positive potentials with an increase in the concentration of MV^{2+}. In the concentration range of (0.1—5) mM, the E_p of the prepeak on DPP was almost independent of the drop time (t_d) and the sampling time.

Normal Pulse Polarography. The adsorption waves of normal pulse polarograms varied with the concentration, the initial potential, the sampling time, and the direction of the potential scan. Figure 3 shows the concentration dependence of the NPP of MV.

Forward Scan: Above 0.5 mM, a sharp prewave appeared with the main wave, and the peak potential of the prewave shifted toward positive potentials with the increase in the MV^{2+} concentration. Below 0.5 mM, the prewave disappeared and a single wave was observed. The limiting current of the main wave or the single wave was proportional to $h^{1/2}$ and $t_s^{-1/2}$ throughout the concentration range of (0.01—5) mM, where h is the height of the mercury column. Below 0.25 mM, $E_{1/2,s}$ shifted by about 0.2 V toward the positive potential from $(E^{0'})_{MV}$, while at concentrations higher than 0.4 mM, the $E_{1/2,s}$ and the E_p of the prewave were not far from $(E^{0'})_{MV}$. The dependence of $E_{1/2,s}$ on E_{in} was observed only in the concentration range of (0.1—0.3) mM, in the range of E_{in} at −(0.3—0.5) V, and with a short t_s (Table 1). The drop time did not affect $E_{1/2,s}$ (Table 1).

Reverse Scan: A sharp postwave appeared throughout the measured concentration range, and the peak potential of the postwave shifted toward positive potentials with an increase in the concentration of MV^{2+}. The peak potential of the postwave on the reverse scan was always more positive than that of the

Table 1. Dependence of $E_{1/2,s}$ on E_{in}, t_d, and t_s[a)]

E_{in}	t_d	$E_{1/2,s}$ / mV		
V	s	t_s / ms		
		30	50	70
0	1	—	−667	—
0	2	−585	−667	−680
0	4	−587	−666	−680
−0.1	4	−588	−663	−680
−0.2	4	−595	−667	−680
−0.3	2	−630	−677	−680
−0.3	4	−630	−677	−680
−0.3	8	−630	—	—
−0.4	4	−672	−677	−680
−0.5	4	−677	−677	−680

a) The solution is 0.28 mM MV^{2+} in 0.1 M of a phosphate buffer solution (pH 7.0). The scan rate is 2 mV s^{-1}.

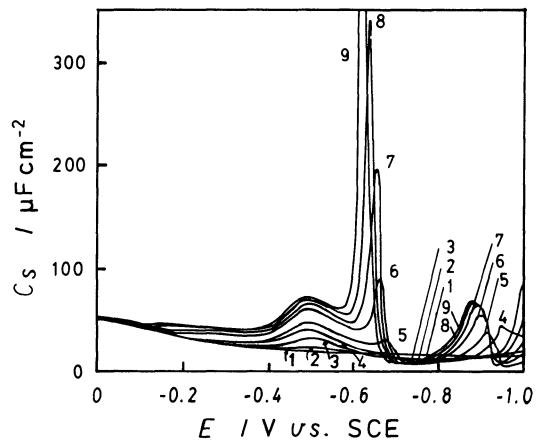

Fig. 4. Differential capacities of methyl viologen at mercury electrode in a 0.1 M phosphate buffer solution (pH 7.0). The concentrations are (1): 0 M, (2): 10 μM, (3): 50 μM, (4): 0.1 mM, (5): 0.25 mM, (6): 0.5 mM, (7): 1 mM, (8): 2 mM, and (9): 5 mM. The scan rate is 2 mV s^{-1}, the drop time 4 s, the a.c. frequency 1 kHz, and the amplitude of a.c. voltage 5 mV.

prewave on the forward scan, and the potential difference between these peaks increased with the decrease in the MV^{2+} concentration. The peak potential of the postwave was independent of t_s and t_d.

a.c. Polarography. Figure 4 shows the differential capacity (C_s) of the mercury electrode in various concentrations of MV^{2+}. Figure 5 shows the variation in C_s with respect to the a.c. frequency. The height of the C_s peak in the vicinity of $(E^{0'})_{MV}$ increased rapidly with the increase in the MV^{2+} concentration and with the decrease in the a.c. frequency. This C_s-peak potential shifted toward positive potentials with an increase in the concentration of MV^{2+}. A broad and symmetric C_s peak ($W_{1/2}$=about 120 mV) was observed at −0.49 V throughout the measured concentration range of (0.01—5) mM. The height of the C_s peak at −0.49 V

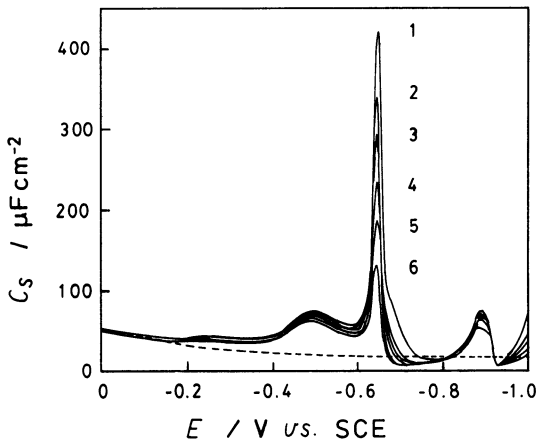

Fig. 5. Frequency dependence of differential capacities of 1 mM MV^{2+} in a 0.1 M phosphate buffer solution (pH 7.0). a.c. frequencies are (1): 100 Hz, (2): 200 Hz, (3): 300 Hz, (4): 500 Hz, (5): 1 kHz, and (6): 2 kHz. (-----): A 0.1 M phosphate buffer solution at 1 kHz (C_s is independent of the a.c. frequency). Other conditions are given in Fig. 4.

Table 2. Amounts of Adsorbed MV^{2+} and $MV^{+\cdot}$ on a Mercury Electrode

Concentration[a]	$\Gamma_{MV^{2+}}$[b]		$\Gamma_{MV^{+\cdot}}$[b]	
	10^{-10} mol cm^{-2}		10^{-10} mol cm^{-2}	
mM	t_d		t_d	
	s		s	
	2	4	2	4
2.3	1.3	1.3	4.0	4.0
1.0	0.93	0.99	3.9	4.0
0.75	0.81	0.84	3.8	3.9
0.5	0.61	0.59	3.8	4.0
0.25	0.47	0.48	3.7	3.9
0.15	0.43	0.45	—	3.8
0.1	0.39	0.45	2.9	3.5

a) Concentrations of methyl viologen in 0.1 M of a phosphate buffer solution (pH 7.0). b) $\Gamma_{MV^{2+}}$ and $\Gamma_{MV^{+\cdot}}$ are the amounts of the adsorbed MV^{2+} and $MV^{+\cdot}$ molecules which were determined by means of potential-step chronocoulometry from −0.3 V to −0.8 V and from −0.8 V to −0.3 V, respectively.

varied slightly with the a.c. frequency and approached a saturation value at concentrations higher than 5 mM. The peak potential at −0.49 V was almost independent of both the concentration of MV^{2+} and the a.c. frequency. The increase in the MV^{2+} concentration led to the depression of C_s in the potential range of −(0.7—0.8) V, and C_s reached a minimum value of 8 μF cm^{-2} in the concentration range of (0.2—1) mM.

The resistive component of the alternating current (R_s) also depended markedly on the concentration of MV^{2+} and the a.c. frequency in the vicinity of $(E^{0'})_{MV}$. At −0.49 V, R_s was almost independent of the concentration of MV^{2+} and the a.c. frequency, and R_s was almost equal to R_{sol}, where R_{sol} was the solution resistance. At −0.65 V in 1 mM of the MV^{2+} solution, the phase angle of the faradaic impedance plot obtained by using the Randles-Ershler equivalent circuit exceeded 45°.

Potential-Step Chronocoulometry. The amounts of MV^{2+} and $MV^{+\cdot}$ adsorbed on the mercury electrode at −0.3 and −0.8 V were evaluated by means of potential-step chronocoulometry.[40]

The amounts of the adsorbed redox species were calculated by the use of

$$(Q_{total})_{t=0} = n_e FS\Gamma + Q_{dl}, \quad (1)$$

where $(Q_{total})_{t=0}$ was the intercept of Q_{total} vs. the $t^{1/2}$ plot; Q_{total}, the total electric charge from time $t=0$ to t; n_e, the number of electrons involved in the redox reaction; S, the area of the electrode; Γ, the surface concentration of adsorbed redox species, and Q_{dl}, the capacitive charge of the double layer. The interfacial capacitance of the electrode covered by methyl viologen, Q_{dl}, was assumed to be equal to that covered by 4,4′-bipyridyl, which is electrochemically stable in the stepped potential range ($E_{1/2}$=−1.06 V)[41] and which has a structure analogous to that of methyl viologen. Table 2 shows the amounts of MV^{2+} and $MV^{+\cdot}$ molecules adsorbed on the mercury electrode, as calculated from Eq. 1.

Discussion

Formal Potential and Diffusion Coefficient of Methyl Viologen. The formal potentials of the $MV^{2+/+\cdot}$ couple in 0.1 M of a phosphate buffer solution at pH 7.0, as obtained by cyclic voltammetry, classical d.c. polarography, and differential pulse polarography, were −(0.680±0.005) V, −(0.682±0.002) V, and −(0.683±0.007) V, respectively. These values were in agreement with the formal potentials of methyl viologen reported in the literatures.[4,5]

Both the diffusion coefficients of MV^{2+} and $MV^{+\cdot}$ which were calculated by the Cottrell equation from NPP, were 4.4×10^{-6} cm^2 s^{-1}.

Adsorption of MV^{2+} Molecules. In the analysis of C_s vs. E curves of methyl viologen obtained by a.c. polarography, Pospisil et al.[3,25] and Grachev et al.[8] have reported that the C_s peak at about −0.49 V is attributable to an adsorption-desorption process of MV^{2+}, for this peak is greatly stretched out along the potential axis, the peak potential is much more positive than $(E^{0'})_{MV}$, and no faradaic wave is observed at about −0.49 V in classical d.c. polarograms. As is shown in Table 2, however, the amount of MV^{2+} molecules adsorbed at −0.3 V is about 1×10^{-10} mol cm^{-2} in 1 mM of a MV^{2+} solution. That is, MV^{2+} has already been adsorbed on a mercury electrode at the foot of the positive side of this C_s peak. The height of the C_s peak is practically independent of the a.c. frequency, and R_s in the vicinity of −0.49 V is equal to R_{sol}. Since the faradaic impedance of a reversible surface redox reaction of the adsorbed species is inde-

pendent of the a.c. frequency,[35,42-44] it is probable that the C_s peak at −0.49 V is attributable to the reversible redox reaction of the adsorbed species and that a repulsive interaction between the adsorbed redox species gives rise to a broad peak.[45,46] In the present NPP study, on the forward scan below 0.25 mM, we have found a diffusion-controlled faradaic wave with a half-wave potential close to −0.49 V, the value at which the broad C_s peak was observed in a.c. polarograms. These results strongly suggest that the C_s peak at −0.49 V is not an adsorption-desorption peak, but the faradaic pseudo-capacitive peak due to the adsorbed MV^{2+} and the adsorbed $MV^{+\cdot}$.

It is probable that the adsorption of MV^{2+} on a positively charged mercury electrode is due to the π-electron interaction between adsorbed molecules and a mercury electrode, which has been reported by Frumkin and Damaskin,[47] and others.[48-56] Moreover, it has been reported that aromatic cations can also be adsorbed on electrodes at more positive potentials than the potential of zero charge of the mercury electrode by means of the π-electron interaction.[8,32,36,57,58]

C_s Peak in the Vicinity of $(E^{0'})_{MV}$. Grachev et al.[8] surmised that, in a.c. polarograms of MV, the C_s peak in the vicinity of $(E^{0'})_{MV}$ was observed only in the narrow concentration range of (0.1—0.2) mM because the first reduction step of MV^{2+} becomes irreversible because of the inhibition by both the adsorbed MV^{2+} molecules in the MV^{2+} concentrations lower than 0.1 mM and the adsorbed $MV^{+\cdot}$ molecules in the MV^{2+} concentrations higher than 0.2 mM. However, both the present and previous studies[2-5,11] have proved that the first reduction step of MV^{2+} is not irreversible, even at the concentrations higher than 0.2 mM. As is shown in Fig. 6, the C_s peak potential in the vicinity of $(E^{0'})_{MV}$ in a.c. polarograms is almost identical with the potential of the prewave in classical d.c. and differential pulse polarograms. It is clear in Fig. 4 that the C_s peak in the vicinity of $(E^{0'})_{MV}$ did not disappear, but shifted toward positive potentials with an increase in the concentration of MV^{2+}.

Orientation of MV^{2+} and $MV^{+\cdot}$. Pospisil et al.[3,25] reported that the marked depression of C_s over −(0.7—0.8) V is caused by a complete coverage of the mercury electrode by $MV^{+\cdot}$ and that the C_s peak at −0.9 V is due to the reorientation of the adsorbed $MV^{+\cdot}$ from flat to vertical.

As is shown in Table 2, the maximum surface concentration of adsorbed $MV^{+\cdot}$ molecules, as determined by potential-step chronocoulometry at −0.8 V, was $(4.0\pm0.1)\times10^{-10}$ mol cm^{-2}. Figure 7 shows the structure of methyl viologen. The area occupied by one molecule adsorbed on an electrode (S_{ad}) can be estimated from the van der Waals radii. If methyl viologen is oriented vertically on the electrode, and if the methyl group of MV can rotate freely around the C-N sigma-bond axis,[59] S_{ad} is estimated to be 34 Å^2 per molecule. If hexagonal array is considered in addition

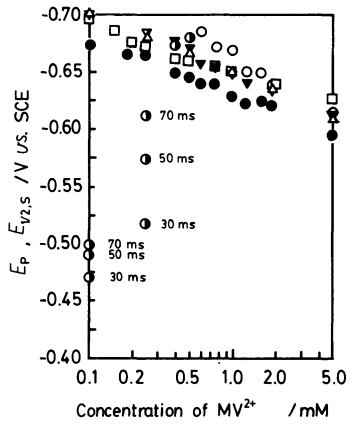

Fig. 6 Concentration dependence of E_p and $E_{1/2,s}$ of methyl viologen. The values of E_p are plotted as (○) for NPP on the forward scan, (●) for NPP on the reverse scan, (□) for a.c. polarograms, (△) for DPP, and (▼) for classical d.c. polarograms. The values of $E_{1/2,s}$ are plotted as (◑) for NPP on the forward scan and (▽) for classical d.c. polarograms. The conditions of measurements are given in Fig. 2—4.

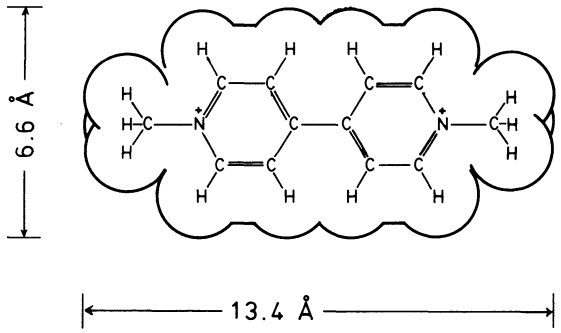

Fig. 7. Structure of methyl viologen.

to a vertical orientation, S_{ad} becomes 38 Å^2 per molecule, which corresponds to 4.4×10^{-10} mol cm^{-2} for the maximum surface concentration (Γ_m). If methyl viologen is oriented flat on an electrode, S_{ad} becomes 88 Å^2 per molecule, which corresponds to 1.9×10^{-10} mol cm^{-2} for Γ_m. If the twisting by 37.2° between two pyridyl rings is considered in addition to a flat orientation, S_{ad} becomes 84 Å^2 per molecule, which corresponds to 2.0×10^{-10} mol cm^{-2} for Γ_m. The good agreement between the measured and the calculated maximum surface concentrations suggests that adsorbed $MV^{+\cdot}$ molecules are oriented vertically, at least in the potential region of −(0.7—0.8) V (cf. Fig. 4). On the other hand, the maximum surface concentration of MV^{2+} has not yet been attained at −0.3 V, as is shown in Table 2 (probably because of a repulsive interaction between adsorbed MV^{2+} molecules) and the orientation of the MV^{2+} molecules adsorbed at a positively charged electrode by means of π-electron interaction is considered to be flat rather than vertical.[43,44,47-58]

Orientation Change of Adsorbed $MV^{+\cdot}$ Molecules. The findings that the C_s peak with the symmetric

shape[37,46] at −0.49 V is independent of the a.c. frequency and that the resistive component at −0.49 V is equal to the solution resistance[44] suggest a surface redox reaction between the adsorbed MV^{2+} molecules and the adsorbed $MV^{+\cdot}$ molecules without the reorientation of the adsorbed species in the vicinity of −0.49 V. If $MV^{+\cdot}$ molecules with a flat orientation are adsorbed on the mercury electrode much more strongly than MV^{2+} molecules (that is, if the ratio of the adsorption coefficient of $MV^{+\cdot}$ to that of MV^{2+} is higher than 10^3), it would be expected that a faradaic prewave would appear at a potential about 0.2 V more positive than $(E^{0'})_{MV}$.

The potential step from the initial potential at which only MV^{2+} molecules have been adsorbed to about −0.49 V gives rise to the formation of adsorbed $MV^{+\cdot}$ at the electrode. A faradaic current and consequently, the $E_{1/2,s}$ are determined by the interfacial concentration gradient and by the surface concentration change of the redox species at the time when the current is sampled.[39] That is, the $E_{1/2,s}$ depends on the t_s, the bulk concentration, and the adsorption states of the redox species at E_{in}. In NPP with a short sampling time at lower concentrations of MV^{2+}, an adsorption wave which is diffusion-controlled can be observed. In NPP at higher concentrations of MV^{2+} and with a long sampling time, and in the differential pulse and the tast polarographic techniques where the electrode potential is kept practically at the sampling potential during the drop time, the amount of the adsorbed $MV^{+\cdot}$ at −0.49 V approaches the value at the adsorption equilibrium or the saturation value. Consequently, the interfacial concentration would be rehomogenized[35] and the adsorption current would decay and would be apt to be overlooked when the current is sampled. On the other hand, in a.c. polarography, a faradaic pseudo-capacitive peak due to the adsorbed MV^{2+} and the adsorbed $MV^{+\cdot}$ molecules can be observed, and also, in cyclic voltammetry, an adsorption peak can be observed provided that the eletrode potential where the $MV^{+\cdot}$ molecules are not adsorbed is chosen for the initial potential.

At concentrations higher than 0.5 mM, as the electrode potential approaches $(E^{0'})_{MV}$, the surface concentration of the adsorbed $MV^{+\cdot}$ molecules increases so abruptly that a reorientation of adsorbed $MV^{+\cdot}$ molecules from flat to vertical takes place.[53,54] The vertical orientation makes possible an attractive interaction between adsorbed $MV^{+\cdot}$ molecules, which causes the further adsorption of $MV^{+\cdot}$ and leads to a sharp adsorption peak. The increase in the bulk concentration of MV^{2+} gives rise to the increase in the interfacial concentration of $MV^{+\cdot}$ after the reduction by a potential step, and the surface concentration of the adsorbed $MV^{+\cdot}$ molecules will be sufficient to change the orientation from flat to vertical at a more positive potential than the potential where the reorientation takes place at lower concentrations of MV^{2+}. It is probable that the positive shift of the peak potential with an increase in the MV^{2+} concentration shown in Fig. 6 is to be attributed to the concentration dependence of the potential at which the reorientation of adsorbed $MV^{+\cdot}$ molecules occurs.

Parry and Parsons[50] have reported that the orientation of *p*-toluenesulfonate adsorbed on a mercury electrode changes from flat at lower concentrations to vertical at higher concentrations, and that the flat orientation accelerates a repulsive interaction between adsorbed *p*-toluenesulfonate molecules, and the vertical orientation, an attractive interaction. Similar discussions of the relation between an orientation and the interaction constants of redox species have been reported by Ershler et al.[60] and others.[48,49,55,56,61,62] Laviron[32] has reported that, in cyclic voltammetry, *trans*-1,2-di(4-pyridyl)ethylene adsorbed on a mercury electrode displays a similar orientation change with the concentration and that the vertical orientation of the redox molecules at the electrode surface causes an attraction force between them which leads to a sharp adsorption peak.

The abrupt change in the orientation of the adsorbed $MV^{+\cdot}$ molecules at the electrode surface leads to the strong frequency dependence of the sharp C_s peak in the vicinity of $(E^{0'})_{MV}$ (Fig. 5). In Fig. 5, the main C_s peak is not observed because of the mergence with the larger adsorption C_s peak. At 6.4 Hz, the appearance of a shoulder corresponding to the main faradaic C_s peak on the negative potential side of a larger C_s peak has been reported.[3] At concentrations lower than 50 μM, no C_s peak appears in the vicinity of $(E^{0'})_{MV}$ because the interfacial concentration of the redox species is negligible compared to the surface concentration of these species because of the depletion of the interfacial concentration as a result of the strong adsorption of the redox species.

In the reverse scan of NPP, the surface concentration of $MV^{+\cdot}$ molecules pre-adsorbed at the initial potential is so high that the adsorbed $MV^{+\cdot}$ molecules are already oriented vertically, even at 0.1 mM (cf. Table 2). The potential step from the initial potential, where the adsorbed $MV^{+\cdot}$ molecules are oriented vertically, to the anodic potential always leads to an orientation change from vertically adsorbed $MV^{+\cdot}$ molecules to flat adsorbed MV^{2+} molecules. This orientation change leads to the situation in which a sharp postpeak always appears over the measured concentration range and the postpeak potential always shifts toward positive potentials with an increase in the concentration.

In the forward scan of NPP, the direction of the shift of the $E_{1/2,s}$ with the concentration in the lower concentration range (<0.5 mM) is opposite to the shift of the prepeak potential with the concentration in the higher concentration range (>0.5 mM). This is probably caused by the change in the orientation of the adsorbed $MV^{+\cdot}$ at the electrode surface and the change in the interaction between adsorbed $MV^{+\cdot}$ molecules. The

potential difference between the prepeak for the forward scan and the postpeak for the reverse scan which is observed at concentrations higher than 0.5 mM probably originates from both the sigmoid-type adsorption isotherm with the strongly attractive interaction between the adsorbed $MV^{+\cdot}$ molecules and the difference between the S_{ad} values of MV^{2+} and $MV^{+\cdot}$ molecules, as has been discussed by Laviron.[37] The peculiar adsorption behavior of methyl viologen is simulated by the digital simulation of the normal pulse polarograms based on the Frumkin-type Flory-Huggins isotherm, which will be published in a subsequent paper.

The present work was supported by a Grant-in-Aid for Scientific Research No. 5670031 from the Ministry of Education, Science and Culture.

References

1) C. L. Bird and A. T. Kuhn, *Chem Soc. Rev.*, **10**, 49 (1981).
2) J. Volke, *Collect. Czech. Chem. Commun.*, **33**, 3044 (1968).
3) L. Pospisil, J. Kuta, and J. Volke, *J. Electroanal. Chem. Interfacial Electrochem.*, **58**, 217 (1975).
4) R. M. Elofson and R. L. Edsberg, *Can. J. Chem.*, **35**, 646 (1957).
5) E. Steckhan and T. Kuwana, *Ber. Bunsenges. Phys. Chem.*, **78**, 253 (1974).
6) E. M. Kosower and J. L. Cotter, *J. Am. Chem. Soc.*, **86**, 5524 (1964).
7) H. T. Van Dam and J. J. Ponjee, *J. Electrochem. Soc.*, **121**, 1555 (1974).
8) V. N. Grachev, S. I. Zhdanov, and G. S. Supin, *Sov. Electrochem.*, **14**, 1180 (1978).
9) G. Hauska, "Photosynthesis 1. Artificial Acceptors and Donors," in "Encyclopedia of Plant Physiology, New Series," Springer-verlag (1977), Vol. 5, Chap. 15.
10) A. B. Bocarsly, D. C. Bookbinder, R. N. Dominey, N. S. Lewis, and M. S. Wrighton, *J. Am. Chem. Soc.*, **102**, 3683 (1980).
11) K. Kobayashi and K. Niki, *Chem. Lett.*, **1982**, 829.
12) Y. M. Tricot, D. N. Furlong, W. H. F. Sasse, P. Daivis, I. Snook, and W. Van Megen, *J. Colloid Interface Sci.*, **97**, 380 (1984).
13) P. Cuendet, M. Gratzel, and M. L. Pelaprat, *J. Electroanal. Chem. Interfacial Electrochem.*, **181**, 173 (1984).
14) W. J. Albery and A. J. Mcmahon, *J. Electroanal. Chem. Interfacial Electrochem.*, **182**, 1 (1985).
15) I. F. Chang, B. L. Gilbert, and T. I. Sun, *J. Electrochem. Soc.*, **122**, 955 (1975).
16) D. J. Barclay, C. L. Bird, and D. H. Martin, *J. Electronic Materials*, **8**, 311 (1979).
17) M. Yamana and T. Kawada, *Nippon Kagaku Kaishi*, **1977**, 941.
18) S. Fletcher, L. Duff, and R. G. Barradas, *J. Electroanal. Chem. Interfacial Electrochem.*, **100**, 759 (1979).
19) J. Bruinink and P. van Zanten, *J. Electrochem. Soc.*, **124**, 1232 (1977).
20) M. Ito and T. Kuwana, *J. Electroanal. Chem. Interfacial Electrochem.*, **32**, 415 (1971).
21) F. Rauwel and D. Thevenot, *J. Electroanal. Chem. Interfacial Electrochem.*, **75**, 579 (1977).
22) S. D. Varfolomeev, A. I. Yaropolov, I. V. Berezin, M. R. Tarasevich, and V. A. Bogdanovskaya, *Bioelectrochem. Bioenerg.*, **4**, 314 (1977).
23) J. F. Stargardt, F. M. Hawkridge, and H. L. Landrum, *Anal. Chem.*, **50**, 930 (1978).
24) B. Zinger and L. L. Miller, *J. Electroanal. Chem. Interfacial Electrochem.*, **181**, 153 (1984).
25) L. Pospisil and J. Kuta, *J. Electroanal. Chem. Interfacial Electrochem.*, **90**, 231 (1978).
26) C. A. Melendres, P. C. Lee, and D. Meisel, *J. Electrochem. Soc.*, **130**, 1523 (1983).
27) R. Rossetti, S. M. Beck, and L. E. Brus, *J. Am. Chem. Soc.*, **106**, 980 (1984).
28) B. Beden, O. Enea, F. Hahn, and C. Lamy, *J. Electroanal. Chem. Interfacial Electrochem.*, **170**, 357 (1984).
29) R. H. Wopshall and I. Shain, *Anal. Chem.*, **39**, 1514 (1967).
30) G. C. Barker and J. A. Bolzan, *Z. Anal. Chem.*, **216**, 215 (1966).
31) A. M. Hartley and G. S. Wilson, *Anal. Chem.*, **38**, 681 (1966).
32) E. Laviron, *J. Electroanal. Chem. Interfacial Electrochem.*, **52**, 355 (1974).
33) D. R. Canterford, *J. Electroanal. Chem. Interfacial Electrochem.*, **52**, 144 (1974).
34) G. Piccardi, F. Pergola, M. L. Foresti, and R. Guidelli, *J. Electroanal. Chem. Interfacial Electrochem.*, **84**, 235 (1977).
35) E. Laviron, "Voltammetric Methods for the Study of Adsorbed Species," in "Electroanalytical Chemistry," ed by A. J. Bard, Marcel Dekker, New York and Basel (1982), Vol. 12, Chap. 2.
36) M. Heyrovsky, S. Vavricka, and R. Heyrovska, *J. Electroanal. Chem. Interfacial Electrochem.*, **46**, 391 (1973).
37) E. Laviron, *J. Electroanal. Chem. Interfacial Electrochem.*, **63**, 245 (1975).
38) J. B. Flanagan, K. Takahashi, and F. C. Anson, *J. Electroanal. Chem. Interfacial Electrochem.*, **81**, 261 (1977).
39) J. B. Flanagan, K. Takahashi, and F. C. Anson, *J. Electroanal. Chem. Interfacial Electrochem.*, **85**, 257 (1977).
40) F. C. Anson, *Anal. Chem.*, **38**, 54 (1966).
41) A. B. Zahlan and R. H. Linnel, *J. Am. Chem. Soc.*, **77**, 6207 (1955).
42) H. A. Laitinen and J. E. B. Randles, *Trans. Faraday Soc.*, **51**, 54 (1955).
43) A. N. Frumkin and B. B. Damaskin, "Modern Aspect of Electrochemistry," ed by J. O'M Bockris and B. E. Conway, Butterworths, Washington (1964), Vol. 3, Chap. 3.
44) B. B. Damaskin, O. A. Petrii, and V. V. Batrakov, "Adsorption of Organic Compounds on Electrodes," Plenum Press, New York and London (1971), Chap. 2.
45) T. Kakutani and M. Senda, *Bull. Chem. Soc. Jpn.*, **52**, 3236 (1979).
46) E. Laviron, *J. Electroanal. Chem. Interfacial Electrochem.*, **105**, 25 (1979).
47) A. N. Frumkin and B. B. Damaskin, *Pure Appl. Chem.*, **15**, 263 (1967).
48) B. E. Conway and R. G. Barradas, *Electrochim. Acta*, **5**, 319 (1961).
49) R. G. Barradas and B. E. Conway, *Electrochim. Acta*, **5**, 349 (1961).

50) J. M. Parry and R. Parsons, *J. Electrochem. Soc.*, **113**, 992 (1966).
51) R. Parsons, *Rev. Pure Appl. Chem.*, **18**, 91 (1968).
52) E. Blomgren, J. O'M Bockris, and C. Jesch, *J. Electrochem. Soc.*, **65**, 2000 (1961).
53) B. B. Damaskin, *J. Electroanal. Chem. Interfacial Electrochem.*, **21**, 149 (1969).
54) B. B. Damaskin, A. A. Sulvila, S. Ya. Vasina, and A. I. Fedorova, *Sov. Electrtochem.*, **3**, 729 (1967).
55) E. A. Mambetkaziev, S. I. Zhdanov, and B. B. Damaskin, *Sov. Electrochem.*, **8**, 1607 (1972).
56) N. K. Akhmetov, R. I. Kaganovich, E. A. Mambetkaziev, and B. B. Damaskin, *Sov. Electrochem.*, **13**, 236 (1977).
57) R. I. Kaganovich, B. B. Damaskin, and M. A. Suranova, *Sov. Electrochem.*, **7**, 1109 (1971).
58) B. B. Damaskin, *Sov. Electrochem.*, **5**, 561 (1969).
59) D. Guerin-euler, C. Nicollin, C. Sieiro, and C. Lamy, *Mol. Phys.*, **34**, 161 (1977).
60) A. B. Ershler, G. A. Tedoradze, and E. M. Podgaetskii, *Sov. Electrochem.*, **7**, 1041 (1971).
61) E. A. Mambetkaziev, A. M. Shaldybaeva, V. N. Statsyuk, and S. I. Zhdanov, *Sov. Electrochem.*, **11**, 1643 (1975).
62) N. K. Akhmetov, R. I. Kaganovich, B. B. Damaskin, and E. A. Mambetkaziev, *Sov. Electrochem.*, **14**, 1534 (1978).